Probes of soft and hard QCD at LHCb

Emanuele Santovetti([1]), on behalf of the LHCb collaboration
([1]) *Università degli Studi di Roma "Tor Vergata" and INFN*

Summary. — The LHCb experiment is instrumented in the forward region. Due to this, it can provide QCD and electroweak measurements complementary to the other LHC experiments. The W and Z production cross-sections have been measured in proton-proton collisions at $\sqrt{s} = 7$ TeV. The measurements of the production cross section of the $\Psi(2S)$ meson and the Υ mesons are reported. The observation of double charm production are also discussed.

PACS 14.70.Fm,14.70.Hp, – W bosons, Z bosons..
PACS 14.40.Pq – Heavy quarkonia.

1. – Introduction

The LHCb experiment is designed to investigate the properties of the heavy quark sector and aims to study CP-violation processes and rare decays involving b and c hadrons. It can also be used to study QCD and electroweak processes. The bb pair production are strongly correlated at small angle with respect to the beam line, therefore the LHCb detector [1] has been designed as a single-arm forward spectrometer covering a pseudorapidity range $2 < \eta < 5$. The detector consists of a silicon vertex detector, a dipole magnet, a tracking system, two ring-imaging Cherenkov (RICH) detectors, a calorimeter system and a muon system.

The LHCb experiments made several measurements in the soft QCD sector (baryon number transport, strange baryon suppression, charged track multiplicity, inclusive ϕ cross section, etc...) as well as in the quarkonium physics. In these proceedings we will present some of the latest results on electroweak physics (section 2) and quarkonia (section 3).

2. – Electroweak measurements

The W and Z production cross-sections at $\sqrt{s} = 7$ TeV energy are measured using the decays $W \to \mu\nu$, $Z \to \mu\mu$ and $Z \to \tau\tau$. The W production charge asymmetry has been also measured as a function of the lepton pseudorapidity.

This analysis uses $\int \mathcal{L} = (16.5 \pm 1.7)$ pb^{-1} of data, collected during 2010 [2]. This results are recently updated with a larger statistic sample [3].

$Z \to \mu^+\mu^-$ selection. – Concerning the $Z \to \mu\mu$, the events are selected by requiring two well reconstructed muons with a transverse momentum, p_T , greater than 20 GeV/c and lying in the pseudo-rapidity (η) range between 2.0 and 4.5. To further identify $Z \to \mu^+\mu^-$ events, the invariant mass is required to be consistent with Z production by imposing the mass constraint 81 GeV/c^2 , $M_{\mu\mu} < 101$ GeV/c^2. 833 candidate events satisfy these criteria.

$W \to \mu\nu$ selection. – The signature for a W boson is a single isolated high transverse momentum lepton and minimal other activity in the event. As the background contamination is expected to be larger than in Z events, additional criteria to the $p_T > 20$ GeV/c and $2.0 < \eta < 4.5$ requirements are imposed; consistency with the primary vertex and muon isolation. Semi-leptonic B and D meson decays are suppressed by requiring the impact parameter significance of the muon with respect to the primary vertex to be less than 2. Isolation is imposed by demanding that the summed transverse energy in a cone of radius $\sqrt{\Delta\eta^2 + \Delta\phi^2} = 0.5$ around the muon is less than 2 GeV/c. 7624 $W^+ \to \mu^+\nu$ and 5732 $W^- \to \mu^-\nu$ candidates pass these requirements.

A detailed background study is performed: $Z \to \mu^+\mu^-$ where one of the muons goes outside the LHCb geometrical acceptance; $W \to \tau\nu$ and $Z \to \tau\tau$ where one tau decays leptonically inside the detector to a muon; b and c events containing semi-leptonic decays with a muon in the final state; generic QCD events where pions or kaons are mis-identified as muons (decay in flight or punch-through).

The signal yield is estimated by fitting the lepton p_T spectrum to the shapes expected for signal (simulation) and each background class (simulation and data-driven by anti-cuts) in 5 bins of the lepton pseudo-rapidity. The W selected candidates and the result of the fit are shown in Fig. 1 (Right). The fit estimates that $(34 \pm 1)\%$ of the sample is composed by $W^+ \to \mu^+\nu$, $(26 \pm 1)\%$ by $W^- \to \mu^-\nu$ and $(31 \pm 1)\%$ is due to the QCD background.

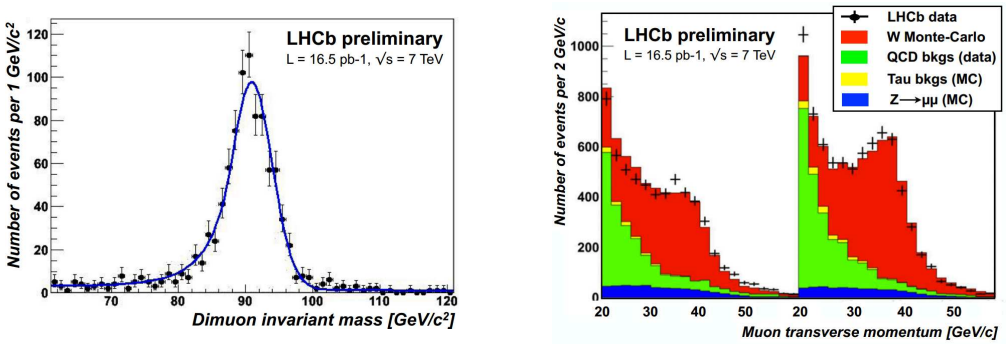

Fig. 1. – (Left) Di-muon invariant mass of Z candidates: data points are fitted to a Crystal Ball function (signal) on an exponential (background). (Right) p_T distribution for negative (left) and positive (right) charged muons.

Results. – The Z and W production cross-sections are measured, with the kinematic requirements above specified, according to the formula:

$$\sigma = \frac{N_{Candidates} - N_{Background}}{\epsilon_{Trigger} \cdot \epsilon_{Tracking} \cdot \epsilon_{\mu-ID} \cdot \epsilon_{Selection} \cdot \int \mathrm{L}} \tag{1a}$$

where all involved efficiencies (trigger, tracking, muon identification and selection) are measured directly from data and cross-checked with simulation. Background estimates, efficiency measurements and luminosity determination are considered as sources of systematic error. Inclusive production cross-sections for Z, W^+ and W^- bosons are determined to be:

$$\sigma(W^+ \to \mu^+\nu) = (1007 \pm 48 \pm 101)\,\text{pb} \tag{2a}$$

$$\sigma(W^- \to \mu^-\nu) = (680 \pm 40 \pm 68)\,\text{pb} \tag{2b}$$

$$\sigma(Z \to \mu\mu) = (73 \pm 4 \pm 7)\,\text{pb} \tag{2c}$$

The differential Z cross-section in 5 bins of the boson rapidity and the W charge asymmetry in 5 bins of lepton pseudo-rapidity are shown in Fig. 2. This measurements can be used to probe the PDF's and test the QCD predictions.

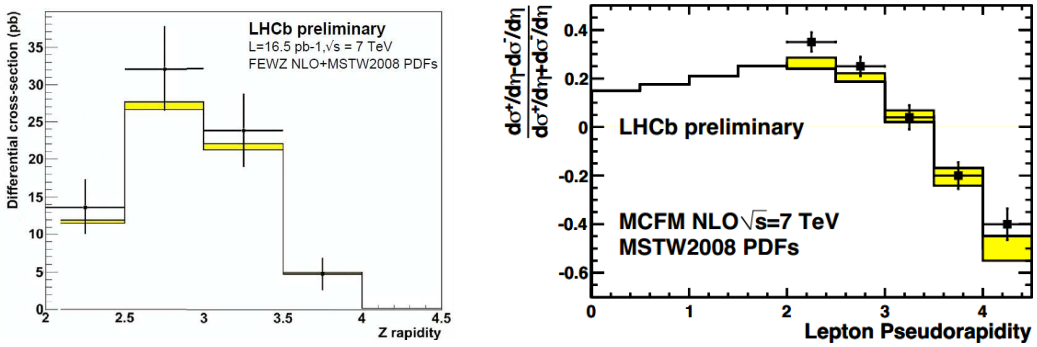

Fig. 2. – (Left) Differential cross-section for Z production in bins of boson rapidity. (Right) W charge asymmetry in bins of lepton pseudo-rapidity. The points are the measured data (statistical and systematic errors combined) compared to the NLO prediction with the MSTW084 PDF set; the yellow band is the theoretical uncertainty.

3. – Quarkonium results

The measurement of $\Psi(2S)$ *meson production at* $\sqrt{s} = 7$ *TeV*. – The differential cross-section for the inclusive production of $\Psi(2S)$ mesons in pp collisions at $\sqrt{s} = 7$ TeV has been measured [4] using an integrated luminosity of 36 pb^{-1}. The decay channels $\Psi(2S) \to \mu^+\mu^-$ and $\Psi(2S) \to (J/\Psi \to \mu^+\mu^-)\pi^+\pi^-$ are reconstructed using prompt $\Psi(2S)$ and $\Psi(2S)$ decaying from a b-hadron (delayed). The separation between the two samples is done using a pseudo-decay-time distribution defined as $t = d_z(M/p_z)$, where d_z is the separation along the beam axis between the $\Psi(2S)$ decay vertex and the primary vertex, M is the nominal $\Psi(2S)$ mass and p_z is the component of its momentum along the beam axis. The polarization of promptly reconstructed $\Psi(2S)$'s is not measured here, therefore a systematic uncertainty is computed separately for the unknown state of the polarization. This does not effect the delayed $\Psi(2S)$. The differential cross-sections for prompt $\Psi(2S)$ and delayed $\Psi(2S)$ mesons are measured in the kinematic range $p_T(\Psi(2S)) < 16$ GeV/c and $2 < y(\Psi(2S)) < 4.5$:

$$\sigma_{prompt}(\Psi(2S)) = 1.44 \pm 0.01(stat) \pm 0.12(syst)^{+0.20}_{-0.40}(pol)\ \mu\text{b} \tag{3a}$$

$$\sigma_b(\Psi(2S)) = 0.25 \pm 0.01(stat) \pm 0.02(sys)\ \mu\text{b} \tag{3b}$$

Recent QCD calculation on the differential cross-sections are found to be in a good agreement with these results as shown in Fig. 3. Combining this result with the LHCb measurement of the J/Ψ cross-section (from b decay) in the same fiducial range [5], the inclusive branching ratio has been determined to be:

$$\mathcal{B}(b \to \Psi(2S)\ X) = (2.73 \pm 0.06(stat) \pm 0.16(syst) \pm 0.24(BR)) \times 10^{-3} \tag{4a}$$

where the last uncertainty is due to the $\mathcal{B}(b \to J/\Psi\ X)$, $\mathcal{B}(J/\Psi \to \mu^+\mu^-)$ and $\mathcal{B}(\Psi(2S) \to e^+e^-)$ branching fraction uncertainties. The later branching fraction is used and justified by the leptons universalities.

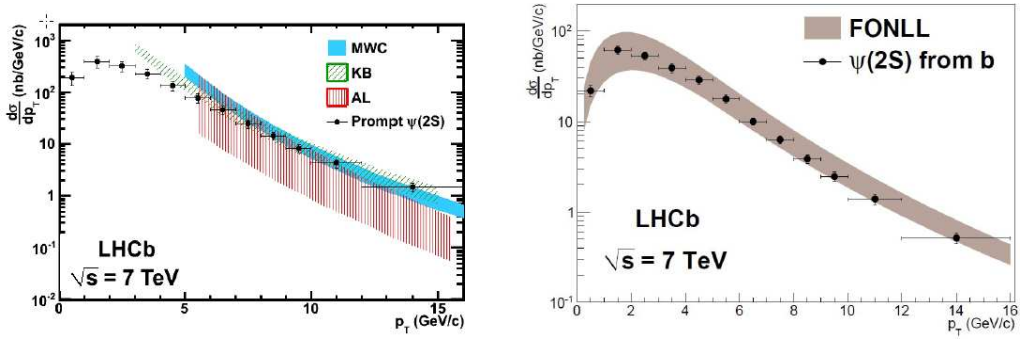

Fig. 3. – (Left) Differential production cross-section vs. p_T for prompt $\Psi(2S)$. The predictions of three non-relativistic QCD models are also shown for comparison. MWC [6] and KB [7] are NLO calculations including colour-singlet and colour-octet contributions. AL [8] is a colour-singlet model including the dominant NNLO terms. (Right) Differential production cross-section vs. p_T for delayed $\Psi(2S)$. The shaded band is the prediction of a FONLL calculation [9].

$\Upsilon(1S)$ *production cross-section.* – The $\Upsilon(1S)$, $\Upsilon(2S)$ and $\Upsilon(3S)$ states have been observed via their decays into two muons with sufficient resolution to separate fully the $\Upsilon(2S)$ and $\Upsilon(3S)$ invariant mass peaks (see Fig. 4 (left)). The $\Upsilon(1S)$ differential production cross-section as a function of $\Upsilon(1S)$ y and p_T has been measured [10] in the fiducial region $pT < 15$ GeV/c and $2.0 < y < 4.5$. The fiducial region has been divided into bins of width 1 GeV/c in p_T and one unit of rapidity (y) and a dataset corresponding to an integrated luminosity of 32.4 pb^{-1} has been used. The $\Upsilon(1S)$ yield has been extracted from a fit to the di-muon invariant mass distribution using a Crystal Ball to model the signal shape and an exponential to model the background shape (see Fig. 4 (left)). The results have been reported under the assumption of unpolarized $\Upsilon(1S)$ and the largest systematic uncertainty comes from this assumption. The measured $\Upsilon(1S)$ production cross-section, integrated over the fiducial region, assuming unpolarized $\Upsilon(1S)$ is $\sigma_{\Upsilon(1S)} = 108.3 \pm 0.7^{+30.9}_{-25.8}$ nb where the first uncertainty is statistical and the second is systematic. The measured $\Upsilon(1S)$ differential production cross-section as a function

of $\Upsilon(1S)$ p_T $(d\sigma/dp_T)$ has been compared with LO and NLO NRQCD, and with NLO and NNLO CS theoretical predictions. The predictions take into account the $\Upsilon(1S)$ feed down from χ_b and $\Upsilon(2S)$ and are in good agreement with data (see, for example, Fig. 4 (right)). The results are allowing for the different rapidity range in good agreement with those obtained by the CMS collaboration [12].

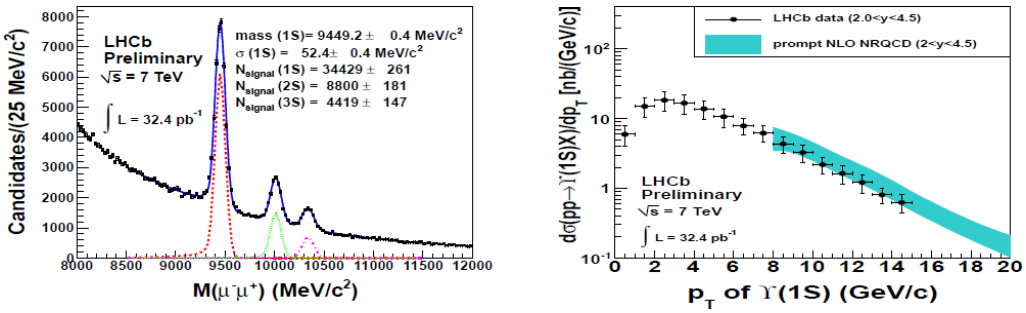

Fig. 4. – (Left) The invariant mass distribution of the selected $\Upsilon \to \mu^+\mu^-$ candidates. The three peaks correspond to the $\Upsilon(1S)$, $\Upsilon(2S)$, and $\Upsilon(3S)$ signals (from left to right). The superimposed curves and the signal yields are the result of the fit. (Right) The measured differential $\Upsilon(1S)$ production cross-section as a function of p_T integrated over y (black dots) compared to the prediction calculated from NRQCD at NLO, including contributions from χ_b and $\Upsilon(2S)$ decays, summing the colour-singlet and colour-octet contributions [11] (coloured band).

Observation of double charm production involving open charm. – The production of a J/Ψ accompanied by open charm and pairs of open charm (C) hadrons are observed [13] in pp collisions at $\sqrt{s} = 7$ TeV using an integrated luminosity of 355 pb^{-1}. Leading order calculation in perturbative QCD and a model including Double Parton Scattering (DPS) [14, 15] give significantly different prediction, $\sigma(J/\Psi\, C) + J/\Psi\bar{C} \sim 18$ nb and ~ 280 nb respectively. The DPS predictions can also be tested through the ratios of cross sections of the charm hadrons involved: in a DPS senario $\sigma(C_1) \times \sigma(C_2)/\sigma(C_1C_2)$ should be equal (twice bigger if $C_1 \neq C_2$) to the effective DPS cross-section measured at the Tevatron [16]. The open charm hadrons considered here are: D^0, D^+, D_s^+ and Λ_c^+, while the $C\bar{C}$ are used as control channels. Selected charged tracks are combined to form $J/\Psi \to \mu^+\mu^-$, $D^0 \to K^-\pi^+$, $D^+ \to K^-\pi^+\pi^+$, $D_s^+ \to K^-K^+\pi^+$ and $\Lambda_c^+ \to pK^+\pi^+$. Subsequently these candidates are combined into $J/\Psi C$, CC and $C\bar{C}$. The combinations are requested to come from the same primary vertex and lie in the rapidity range $2 < y(J/\Psi, C) < 4$ and the p_T range $p_T(J/\Psi) < 12$ GeV/c and 3 GeV/c$< p_T(C) < 12$ GeV/c. In addition a flight distance $c\tau > 100$ μm is required for the C.

Signals with a statistical significance over five standard deviations have been observed for the four $J/\Psi\, C$, for six CC modes: D^0D^0, D^0D^+, $D^0D_s^+$, $D^0\Lambda_C^+$, D^+D^+ and $D^+D_s^+$, and for seven $C\bar{C}$ channels: $D^0\bar{D}0$, D^0D^-, $D^0D_s^-$, $D^0\bar{\lambda}_c^-$, D^+D^-, $D^+D_s^-$ and $D^+\bar{\Lambda}_c^-$. In Fig. 5 the cross-sections are shown on the left and the DPS fraction on the right. Results favour the DPS model using the effective cross-section measured at Tevatron, which is also favoured with the absence of azimuthal and rapidity correlations. The transverse momentum of these events has also been studied. In the $J/\Psi C$ case we can see an harder $p_T^{J/\Psi}$ spectra compared to the prompt J/Ψ production.

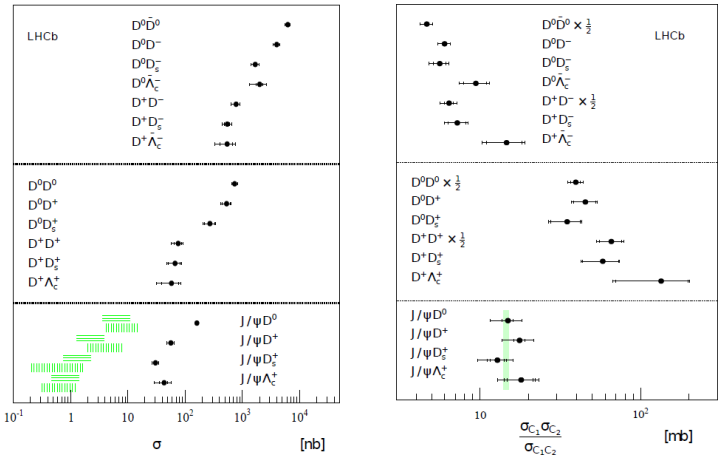

Fig. 5. – (Left) Measured cross-sections $\sigma_{J/\Psi C}$, σ_{CC} and $\sigma_{C\bar{C}}$ (points with error bars) compared, in $J/\Psi C$ channels, to the calculations in Refs. [17] (vertical hatched areas) and Ref. [18] (horizontal hatched areas). The inner error bars show the statistical uncertainty whilst the outer error bars show the sum of the statistical and systematic uncertainties in quadrature. (Right) Measured ratios $\sigma(C_1) \times \sigma(C_2)/\sigma(C_1C_2)$ (points with error bars) in comparison with the expectations from DPS using the cross-section measured at Tevatron for multi-jet events (light green shaded area). For the D^0D^0, $D^0\bar{D}^0$, D^+D^+ and D^+D^- cases the ratios are rescaled with the symmetry factor of one half. The inner error bars show the statistical uncertainty whilst the outer error bars show the sum of the statistical and systematic uncertainties in quadrature. For the $J/\Psi C$ case the outermost error bars correspond to the total uncertainties including the uncertainties due to the unknown polarization of the prompt J/Ψ mesons.

REFERENCES

[1] The LHC*b* Collaboration, A.A. Alves et al., *JINST 3*, **13** (2008) s08005
[2] The LHC*b* Collaboration, arXiv:1204.1620 (submitted to EPJ)
[3] The LHC*b* Collaboration, LHCb-CONF-2011-039
[4] The LHC*b* Collaboration, arXiv:1204.1258 (submitted to EPJ)
[5] The LHC*b* Collaboration, Eur. Phys. J. C **71** (2011) 1645
Eur. Phys. J. C 71 (2011) 1645
[6] Y.Q. Ma, K. Wang and K.T. Chao, arXiv:hep-ph/1012.1030
[7] B. Kniehl and M. Butenschön, Phys. Rev. Lett. **106**, (2011)
[8] Phys. Rev. Lett **101**, 152001 (2008) and Eur. Phys J. C **61**, 693 (2009)
[9] JHEP **9805**, 007 (1998) and JHEP **0407**, 033 (2004)
[10] The LHC*b* Collaboration, Eur. Phys. J. C (2012) **72**:2025
[11] K. Wang, Y.Q. Ma, K.T. Chao, private communication
[12] The CMS Collaboration, arXiv:1012.5545v1
[13] The LHC*b* Collaboration, arXiv:1205.0975 (sbmitted to JHEP)
[14] Phys. Rev. D **57**, 4385 (1998) and Phys. Rev. D **73**, 074021 (2006)
[15] Phys. Rev. Lett. **107**, 082002 (2011), Phys. Rev. B **705**, 116 (2011) and arXiv:1106.2184
[16] CDF Collaboration, Phys. Rev. D **56**, 3811 (1997)
[17] Phys. Rev. D **57**, 4385 (1998) and Phys. Rev. D **73**, 074021 (2006)
[18] J.P. Lansberg, Eur. Phys. Rev. J. C **61**, 693 (2009)